JCTC Journal of Chemical Theory and Computation

Article

pubs.acs.org/JCTC

Assessment of Perturbative Explicitly Correlated Methods for Prototypes of Multiconfiguration Electronic Structure

Luke B. Roskop,[†] Liguo Kong,[‡,§] Edward F. Valeev,[‡] Mark S. Gordon,[†] and Theresa L. Windus*[,†]

[†]Department of Chemistry, Iowa State University, Ames, Iowa 50010, United States

[‡]Department of Chemistry, Virginia Tech, Blacksburg, Virginia 24061, United States

Supporting Information

ABSTRACT: The performance of the $[2]_S$ and $[2]_{R12}$ universal perturbative corrections that account for one- and many-body basis set errors of single- and multiconfiguration electronic structure methods is assessed. A new formulation of the $[2]_{R12}$ methods is used in which only strongly occupied orbitals are correlated, making the approach more amenable for larger computations. Three model problems are considered using the aug-cc-pVXZ (X = D,T,Q) basis sets: the electron affinity of fluorine atom, a conformational analysis of two Si_2H_4 structures, and a description of the potential energy surfaces of the X $^1\Sigma_g^+$, a $^3\Pi_u$, b $^3\Sigma_g^-$, and A $^1\Pi_u$ states of C_2. In general, the $[2]_{R12}$ and $[2]_S$ corrections enhance energy convergence for conventional multireference configuration interaction (MRCI) and multireference perturbation theory (MRMP2) calculations compared to their complete basis set limits. For the electron affinity of the F atom, $[2]_{R12}$ electron affinities are within 0.001 eV of the experimental value. The $[2]_{R12}$ conformer relative energy error for Si_2H_4 is less than 0.1 kcal/mol compared to the complete basis set limit. The C_2 potential energy surfaces show nonparallelity errors that are within 0.7 kcal/mol compared to the complete basis set limit. The perturbative nature of the $[2]_{R12}$ and $[2]_S$ methods facilitates the development of a straightforward text-based data exchange standard that connects an electronic structure code that can produce a two-particle density matrix with a code that computes the corrections. This data exchange standard was used to implement the interface between the GAMESS MRCI and MRMP2 codes and the MPQC $[2]_{R12}$ and $[2]_S$ capabilities.

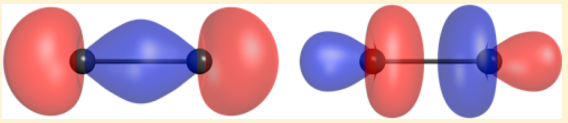

INTRODUCTION

Explicitly correlated R12/F12 methods[1−4] are an effective approach to reduce the basis set incompleteness error (BSIE) of the conventional (i.e., based on Slater determinants) ab initio many-body methods. The primary source of the BSIE is the slow convergence of the atomic basis set within Slater determinant based expansions near the singularities of the interelectronic potential. Although Slater determinants are computationally convenient because of factorization of n-electron matrix elements (Slater−Condon rules), they describe an interelectronic potential that is smooth everywhere, whereas the exact wave functions are known to have cusps wherever the interelectronic potential is singular. When electrons approach one another, the exact wave function is linear in the interparticle distance (r_{ij}) with the coefficient dependent on how the spins of the electrons are coupled:

$$(\partial\hat{\Psi}/\partial r_{ij})_{r_{ij}=0} = \gamma\Psi(r_{ij} = 0) \quad (1)$$

where $\hat{\Psi}$ is the spherically averaged wave function Ψ about the point of coalescence ($r_{ij} = 0$), and $\gamma = 1/2$ for a singlet spin coupled electron pair. The description of the cusp in terms of Slater determinants requires the use of high angular momentum basis functions that causes a steep rise of the computational expense with an increase in the accuracy. An alternative is to augment the Slater determinants with basis functions that describe the cusp directly in terms of the interelectronic distances, r_{ij}, as is done in R12 methods.

All R12 methods involve n-electron ($n > 1$) basis functions that depend on the *correlation factor*, $f(r_{ij})$, a function of the interelectronic coordinate r_{ij} that is used to capture the essential shape of the wave function at short r_{ij}. The three- and four-electron integrals that appear in R12 methods are handled approximately by factorization into two-electron integrals only.[5,6] Robust R12 methods for the single-configurational ground-state wave functions, such as the coupled-cluster singles and doubles (CCSD) approach, have become well-established in the past decade.[7−10] However, R12 methods for multireference (MR) wave functions have not been as thoroughly tested; although several such methods have been introduced, as discussed in the following paragraphs. A better understanding of the strengths and weaknesses of explicitly correlated MR methods is important since MR wave functions are essential for reliable descriptions of chemical species that exhibit near degeneracies which occur in the vicinity of conical intersections, in bond breaking, in free radical chemistry, in electronic excited states, and in unsaturated transition metal compounds.

An early adaptation of single reference R12 methodology to MR wave functions (MR-R12) resulted in the linear R12 multireference configuration interaction (R12-MRCI)[11] method and the linear multireference averaged coupled-pair functional (R12-ACPF)[12] method. These methods augmented the conventional MRCI and ACPF expansions with many terms that

Received: July 29, 2013
Published: November 12, 2013

dx.doi.org/10.1021/ct4006773 | J. Chem. Theory Comput. 2014, 10, 90−101

are linearly dependent on r_{ij}. Because no specialized basis set was used to approximate many-electron integrals, very large orbital basis sets were required and, therefore, applications were limited to atoms and very small molecules. Later Ten-no introduced MRMP2-F12,[13] the first generally applicable MR method to use the modern F12 technology; this method was based on the multireference MP2 approach of Hirao.[14] Ten-no arrived at a practical method by introducing two key advances: (1) the use of fixed-form (i.e., containing no variable parameters aside from the geminal functional form) internally contracted geminal functions, and (2) some additional approximations that are designed to avoid the need for the three-body reduced density matrix (3-RDM). Shiozaki and Werner implemented CASPT2-F12[15] without the additional approximations of Ten-no, thereby requiring the 3-RDM. Since CASPT2 requires at least the 3-RDM, regardless of the formulation, this is not a substantial problem. Shiozaki et al. also extended the approach to (partially) internally contracted MRCI[16] (MRCI-F12) by introducing the internally contracted explicitly correlated terms a priori. Hence, the amplitudes of the conventional wave function are modified because of the coupling.

Many recent developments in multireference methods can be found in the literature. Klopper et al. extended the Mukherjee variant of second-order multireference perturbation theory Mk-MR-PT2[17] to the F12 framework as well.[18,19] Notable advances in the area of MR coupled cluster theory are the explicitly correlated internally contracted MR coupled-cluster singles and double theory (ic-MRCCSD(F12*)[20] and the MR Brillouin−Wigner CCSD-R12 (BW-CCSD-R12) and BW-CCSD-F12 methods.[21]

The present work assesses the performance of a modification of the universal perturbative explicitly correlated approach $[2]_{R12}$[22] developed by Kong and Valeev.[4] Like MRMP2-F12, $[2]_{R12}$ is technically similar to MP2-R12 and only needs a two-particle density matrix. Yet $[2]_{R12}$ can also be applied to more general correlated states than CASSCF without requiring an increase in theoretical complexity; for example, an entire MRCI wave function can be used as the reference and, thus, higher-order basis set incompleteness effects can be treated. Furthermore, methods without an explicit wave function, such as the determinant-based quantum Monte Carlo (QMC) method, have also been augmented with $[2]_{R12}$;[23] emerging Density Matrix Renormalization Group (DMRG)[24] applications could similarly be improved using the $[2]_{R12}$ correction. Because $[2]_{R12}$ is an a posteriori correction, it may be reasonable to assume that when basis set effects are significant, the $[2]_{R12}$ approach may not perform as well as a priori schemes like the MRCI-F12 scheme of Shiozaki and Werner. Hence it is mandatory to document the performance of the $[2]_{R12}$ approach as rigorously as possible. This is also timely in the light of a related development by Yanai and Shiozaki of a canonical transformation of the Hamiltonian using explicitly correlated geminals[25] whose computational cost is comparable to that of $[2]_{R12}$. Note that the Hamiltonian transformation in their approach is state-specific (depends on a reference density), thus it can be viewed as an a priori counterpart to the state-specific a posteriori $[2]_{R12}$ approach.

This paper evaluates the performance of the modified formulation of the explicitly correlated $[2]_{R12}$ correction (and its sister $[2]_S$ basis set correction, see below).

This formulation gains an advantage over the most recent presentation of $[2]_{R12}$ by Kong and Valeev by making a cogent distinction between those orbitals that are correlated using geminals and those orbitals in terms of which the RDMs are expressed. The new approach allows the use of MRCI as the reference while correlating only the strongly occupied orbitals, for example, the active space subset. The present work tests the $[2]_{R12}$ method on a set of prototypical problems that include ground and excited states, and changing numbers of electrons. MRCI- and MRMP2-based methods[14] were used to compute (1) the electron affinity (EA) of fluorine atom and (2) conformational energies of Si_2H_4. An explicitly correlated MRCI approach is also used to compute (3) the potential energy surfaces (PES) for the ground and three lowest-energy excited states of C_2. These test cases provide a critical test of the reliability of the $[2]_{R12}$ and $[2]_S$ BSIE corrections for different applications: the EA of F deals with different electron densities (anion vs neutral species), Si_2H_4 provides a conformational analysis, and C_2 is used to study the dissociation of a chemical bond and relative energies of multiple excited states. $[2]_{R12}$ and $[2]_S$ BSIE corrections are calculated for each of these chemical systems and, where possible, the results are compared to the available experimental data. Timing information for the pilot code is given for a C_2 calculation to provide an idea of the expense of the different parts of the computation.

The newly developed data exchange standard that facilitates the implementation of these corrections for MRCI and MRMP2 via a link between the GAMESS[26] and MPQC[27] programs is described. GAMESS was used to compute the reference CASSCF or MRCI wave functions, and the corresponding MRMP2 correlation energies. GAMESS was also used to generate the MRCI or CASSCF second-order density matrices that were used by MPQC to evaluate the $[2]_{R12}$ and $[2]_S$ BSIE corrections. A similar interface has also been recently developed between the MPQC and MOLCAS[28] programs.

METHOD

The $[2]_{R12}$ method used in this work is similar to the spin-free formulation described in ref 4. However, simple changes have been made for the MRCI reference wave function. These changes reduce the cost of correcting for the higher-order BSIE that occurs because of the coupling of the conventional dynamic correlation effects in the MRCI method with the R12 geminal correlation. Within the $[2]_{R12}$ framework, one has the ability to decide which orbitals are correlated by R12 geminals. These orbitals, referred to herein as geminal orbitals, should be chemically significant (i.e., valence orbitals, orbitals from a MCSCF active space). By only correlating a subset of the finite orbital basis set (OBS), a high degree of accuracy is still achievable at a reduced computational expense. For context, the essential details of the spin-free $[2]_{R12}$ method are briefly described.

For a given reference wave function $|0\rangle$ (e.g., CASSCF, CI, QMC), the $[2]_{R12}$ correction describes the dynamic correlation effects that cannot be described in the determinant space that is generated by the finite OBS. Therefore, the correction is identified with the two-electron basis set incompleteness. Here, "two-electron" is defined with respect to the reference wave function and, thus, can take on n-electron ($n > 2$) meaning with respect to a given determinant. The $[2]_{R12}$ energy correction is evaluated by the second-order Hylleraas functional:

$$\mathcal{H} = 2\langle 0|H^{(1)}|\psi^{(1)}\rangle + \langle \psi^{(1)}|H^{(0)} - E^{(0)}|\psi^{(1)}\rangle \quad (2)$$

where the first-order wave function $|\psi^{(1)}\rangle$ is defined as in ref 4., using the Einstein summation notation:

dx.doi.org/10.1021/ct4006773 | J. Chem. Theory Comput. 2014, 10, 90−101

$$|\psi^{(1)}\rangle = \frac{1}{2} t_{rs}^{pq} (r_{\alpha'\beta'}^{rs} E_{pq}^{\alpha'\beta'} + 2 r_{\alpha' x}^{rs} E_{pq}^{\alpha' x} - 2 r_{\alpha' k}^{rs} (\Gamma^{(-1)})_j^i \Gamma_{pq}^{jk} E_i^{\alpha'}) |0\rangle \tag{3}$$

In this paper, following the same notation as in ref 4, $p/q/r/s/t/u/v/w/o$ refer to the orbitals correlated by R12 geminals (this will usually include only strongly occupied orbitals), $i/j/k$ refer to the occupied orbitals (all orbitals corresponding to nonzero elements of the reference RDMs), x/y refer to the orbitals in the OBS, α'/β' refer to a subset of orbitals from the formal complete basis set (CBS) that are orthogonal to the conventional OBS, and $\kappa/\lambda/\mu$ are the orbitals in the CBS (the union of $\{\alpha'\}$ and the OBS). $E_i^{\alpha'}$ and $E_i^{\alpha'\beta'}$ denote spin-free substitution operators, eq 4, in which $a_p^\dagger$ and a_q are the standard creation and annihilation operators:

$$E_p^q = \sum_{\sigma=\{\alpha,\beta\}} a_{p_\sigma}^\dagger a_{q_\sigma}$$
$$E_{rs}^{pq} = \sum_{\sigma,\tau=\{\alpha,\beta\}} a_{p_\sigma}^\dagger a_{q_\tau}^\dagger a_{s_\tau} a_{r_\sigma} \tag{4}$$

$r_{\kappa\lambda}^{rs}$ is the spin-free matrix element of the correlation factor $(f(r_{12}))$

$$r_{\kappa\lambda}^{rs} = \iint \phi_\kappa(r_1)\, \phi_\lambda(r_2)\, f(r_{12})\, \phi_r(r_1)\, \phi_s(r_2)\, \mathrm{d}r_1\, \mathrm{d}r_2 \tag{5}$$

t_{rs}^{pq} are the geminal coefficients that are fixed according to the rational generator method of Ten-no to satisfy the first-order cusp condition:[6]

$$t_{rs}^{pq} = \frac{3}{8}\delta_r^p \delta_s^q + \frac{1}{8}\delta_s^p \delta_r^q \tag{6}$$

Γ denotes the 1-electron and 2-electron spin-free RDMs of the reference wave function

$$\Gamma_j^i = \langle 0|E_j^i|0\rangle,$$
$$\Gamma_{kl}^{ij} = \langle 0|E_{kl}^{ij}|0\rangle. \tag{7}$$

The α'/β' orbitals are approximated by the complementary auxiliary basis set (CABS) orbitals that are constructed by the CABS+ procedure;[5] the $\kappa/\lambda/\mu$ orbitals are approximated using the union of CABS and OBS orbitals.

In the original applications of the $[2]_{R12}$ method[4,22] every occupied orbital was geminal-correlated (i.e., $\{p\} = \{i\}$ using the orbital notation given after eq 3). An occupied orbital, i, means any orbital in the orbital basis set with nonzero occupancy in the reference wave function (i.e., there is at least one nonzero matrix element of the 1-RDM involving this orbital). For reference wave functions with a significant degree of dynamic electron correlation, many orbitals in the orbital basis are occupied, but only weakly. Because the computational complexity of the $[2]_{R12}$ energy is at least quartic with respect to the number of correlated orbitals, it makes sense to avoid the excessive computational cost of the $[2]_{R12}$ correction by correlating only important (i.e., strongly occupied) orbitals.[4] There are several ways to determine the strongly occupied orbitals, for example, use natural orbitals that have well-defined occupancies. Because only CASSCF-based reference wave functions (MRPT and MRCI) are utilized, the active space is used to define which orbitals are important. Hence, {p} equals the inactive and active orbitals of the CASSCF. Unlike the previous application of $[2]_{R12}$ to MRCI,[4] the MRCI $[2]_{R12}$ correction is calculated using the MRCI (not the CASSCF) density. Therefore, it is important to carefully distinguish the geminal-correlated ($\{p\}$), occupied ($\{i\}$), and orbital ($\{x\}$) indices. For completeness, the full expressions (using Einstein summation notation) for the $[2]_{R12}$ correction are presented here:

$$\mathcal{H}^{(2)} = 2\mathcal{V} + (\mathcal{B}_0 + \mathcal{X} + \Delta) \tag{8}$$

$$\mathcal{V} = \frac{1}{2} t_{rs}^{pq} \Gamma_{pq}^{ij} \left((gr)_{ij}^{rs} - g_{ij}^{xy} r_{xy}^{rs} - g_{ij}^{\alpha' k} \Gamma_k^l r_{\alpha' l}^{rs} \right) \tag{9}$$

$$\mathcal{X} = -t_{rs}^{pq} t_{tu}^{vw} (\Gamma_{vi}^{rs} f_w^i) \left((r^2)_{pq}^{tu} - r_{pq}^{xy} r_{xy}^{tu} - r_{pq}^{\alpha' k} \Gamma_k^l r_{\alpha' l}^{tu} \right) \tag{10}$$

$$\begin{aligned} \mathcal{B}_0 = t_{rs}^{pq} t_{tu}^{vw} \Gamma_{vw}^{rs} \Bigg(& \frac{1}{2} (rTr)_{pq}^{tu} + (r^2)_{pq}^{t\kappa} (hJ)_\kappa^u - r_{pq}^{\mu\lambda} K_\lambda^\kappa r_{\mu\kappa}^{tu} \\ & - r_{pq}^{xy} f_y^z r_{xz}^{tu} - 2 r_{pq}^{yx} f_x^{\alpha'} r_{y\alpha'}^{tu} - \frac{1}{2} r_{pq}^{\beta' k} \Gamma_k^l f_{\beta'}^{\alpha'} r_{\alpha' l}^{tu} \\ & - \frac{1}{2} r_{pq}^{\alpha' k} \Gamma_k^l f_l^\kappa r_{\alpha'\kappa}^{tu} \Bigg) \end{aligned} \tag{11}$$

$$\begin{aligned} \Delta = -(r_{\alpha'\kappa}^{tu} f_i^\kappa t_{tu}^{vw}) (t_{rs}^{pq} r_{pq}^{\alpha' j}) \Bigg[& \Gamma_v^s \left(-\frac{1}{2}\Gamma_{wj}^{ir} + \frac{1}{2}\Gamma_w^i \Gamma_j^r \right. \\ & \left. - \frac{1}{2}\Gamma_w^r \Gamma_j^i \right) + \Gamma_w^s \left(-\frac{1}{2}\Gamma_{jv}^{ir} + \Gamma_v^r \Gamma_j^i - \frac{1}{4}\Gamma_j^r \Gamma_v^i \right) \\ & + \Gamma_v^r (\Gamma_{wj}^{is} - \Gamma_j^s \Gamma_w^i) + \Gamma_w^r \left(-\frac{1}{2}\Gamma_{vj}^{is} + \frac{1}{2}\Gamma_j^s \Gamma_v^i \right) \Bigg] \end{aligned} \tag{12}$$

where r^2, gr, and rTr refer to the two-electron integrals of $(f(r_{12}))^2$, $f(r_{12})/r_{12}$, and $[f(r_{12}), [T_1, f(r_{12})]]$, respectively, and hJ, T, and K refer to the one-electron integrals of the core Hamiltonian plus Coulomb, kinetic energy, and exchange operators, respectively.

The matrix elements in the $[2]_{R12}$ Hylleraas functional were evaluated using the CABS+ approximation[5] and an exponential correlation factor,[29] $f(r_{ij}) = -\gamma^{-1} \exp(-\gamma r_{ij})$ (where γ is set to the recommended value for the particular orbital basis set), is fitted to a linear combination of six Gaussian geminals. *All explicitly correlated MRCI results are computed with the MRCI second-order density, while the CASSCF second-order density is used for explicitly correlated MRMP2 computations.*

Since $[2]_{R12}$ corrects the two-electron basis set incompleteness (correlation energy), the dominant source of residual error becomes the one-electron basis set incompleteness (reference energy). This deficiency is addressed by the perturbative $[2]_S$ correction of Kong and Valeev that accounts for the one-electron BSIE of the reference (CASSCF) energy.[30] In this work the $[2]_S$ corrections were evaluated with the Dyall zeroth-order Hamiltonian.[31]

As an alternative to the $[2]_S$ correction, the one-electron BSIE was estimated as the difference between the CASSCF energy in the basis set being used and the CASSCF/aug-cc-pVQZ[32] energy. This alternative method provides an independent, variational method for obtaining the one-electron BSIE for comparison with the $[2]_S$ correction. The variationally corrected BSIE is then combined with either the aug-cc-pVDZ or the aug-cc-pVTZ MRCI and MRMP2 dynamic correlation energies, defined as $E_{mrx} - E_{casscf}$ (x = CI or MP2) to obtain the total energy. Results using this large basis set reference energy are indicated by a "*" (e.g., MRCI*).

dx.doi.org/10.1021/ct4006773 | J. Chem. Theory Comput. 2014, 10, 90−101

The CBS limit of the correlation energy was estimated via the inverse power expansion[33] of the correlation energy based on the aug-cc-pVTZ and aug-cc-pVQZ basis sets as

$$E_{\mathrm{corr}}(X) = E_{\mathrm{corr}}(\mathrm{CBS}) + AX^{-3} \quad (13)$$

whereas the CBS limit of the CASSCF reference energy was obtained by an exponential extrapolation:[34,35]

$$E_{\mathrm{REF}}(X) = E_{\mathrm{REF}}(\mathrm{CBS}) + Ae^{-bX} \quad (14)$$

All computations in this work were performed using the new interface between the GAMESS and MPQC packages. GAMESS was used to compute the reference/correlation energies, molecular orbitals, and second-order reduced density matrices. MPQC subsequently was used to compute the $[2]_{R12}$ and $[2]_s$ BSIE corrections. Since GAMESS is mostly written in the Fortran 77 programing language and MPQC is primarily written in C++, the data between GAMESS and MPQC is exchanged via human-readable text files containing the two particle reduced density matrix (2-RDM) and the associated metadata (molecular geometry, atomic orbital basis set, and molecular orbitals). The expansion coefficients for each molecular orbital are passed to a disk file in which the atomic and molecular orbital indices are explicitly given. The coordinates are passed in the usual xyz format and are labeled with the appropriate atomic number. To take advantage of the sparsity of the second-order density matrix, only density matrix elements that are above a defined threshold (i.e., 10^{-12}) are printed to disk with each element explicitly labeled with its four orbital indices. All atomic orbital basis set information is sent to disk, which allows MPQC to compute the BSIE corrections independently of GAMESS. A descriptive explanation of the format used for the disk files is presented in the Supporting Information. Alternatively, GAMESS is fully interfaced to MPQC with the MPQC control options passed from GAMESS through the standard argv/argc command line arguments. This allows the two software programs to be run as one application. An example input can be found in the Supporting Information, Figure 1.

Currently, the GAMESS/MPQC interface is limited by the amount of memory that is required to store the 2-RDM. This storage requirement ($\sim g^2n^2/4$ where n is the number of molecular orbitals and g is the number of geminal-correlated orbitals) limits both the GAMESS and MPQC programs. During parallel execution GAMESS is much less impacted by this restriction because it places the 2-RDM into distributed memory, which is memory shared between compute nodes. One final note: the diagonalization of the CI Hamiltonian and the generation of the second-order density matrix in GAMESS are computed in parallel across multiple nodes while the MPQC $[2]_{R12}$ and $[2]_S$ BSIE corrections are currently limited to parallel execution among the cores within a single node.

RESULTS

Electron Affinity of Atomic Fluorine. The determination of EAs can be a difficult test for electronic structure methods because of the lack of cancellation of errors between the electron correlation and relaxation effects upon the attachment of an electron. Therefore the electronic structures of the neutral and ionic species must both be described accurately.[36−38] The purpose of this subsection is to examine the performance of the $[2]_{R12}$ BSIE and $[2]_S$ corrections when applied to the electronic structures of fluorine atom and its anion. Three different CASSCF reference wave functions are used to perform MRCI and MRMP2 computations. The smallest reference active space (ACT-1) is constructed from 9 active orbitals: 1s, 2s, all three 2p, 3s, and all three 3p. For the neutral (anionic) species, the active space included 9 (10) electrons. The second active space (ACT-2) is constructed from the 2s, all three 2p, 3s, all three 3p, and all five 3d orbitals, while the 1s orbital is constrained to be doubly occupied in both the CASSCF and MRCI computations. For ACT-2, there are 7 (8) electrons distributed among the 13 active orbitals for the neutral (anionic) species. The last active space (ACT-3) includes the 1s, 2s, all three 2p, 3s, all three 3p, and all five 3d orbitals (14 orbitals) and contains 9 (10) electrons for the neutral (anionic) species. Both conventional and explicitly correlated MRCI and MRMP2 results are presented. For the ACT-3 reference space, MRCI was only performed with the aug-cc-pVDZ and aug-cc-pVTZ basis sets since the memory requirement for the conventional (uncontracted) MRCI computation is not practical for the aug-cc-pVQZ basis set.

Previously, the EA of F atom was computed with the approximately size extensive R12 MR averaged coupled-pair functional (R12-MRACPF)[39] with a composite basis set (see Table 2 in ref 40) including a relativistic correction and found to be 3.385 eV.[40] Without the relativistic correction the R12-MRACPF EA was found to be 3.398 eV. These EAs are comparable to the CCSD + F12 + "high level correction" value (3.4276 eV)[41] and the experimental value (3.401 eV).[42]

Table 1 displays the MRCI EA values of F atom predicted by the ACT-1, ACT-2 and ACT-3 active spaces (see Supporting Information, Tables 1−3 for total energy values). As expected, the conventional MRCI EA values approach the ACT-1 and ACT-2 CBS limits (3.392 and 3.427 eV, respectively) as the size of the AO basis is increased. Compared to conventional MRCI values, the MRCI + $[2]_{R12}$ EAs are improved at each respective basis set level. Once the $[2]_S$ correction is included (MRCI+$[2]_{R12}$+$[2]_S$), the reported EAs for each basis set using ACT-1 lie within ∼0.02 eV of each other, while the EAs computed with ACT-2 for each basis set lie within ∼0.01 eV of each other. For the aug-cc-pVTZ basis set, the MRCI*+$[2]_{R12}$ errors (compared to CBS) are slightly smaller than those computed by MRCI+$[2]_{R12}$+$[2]_S$. However, the aug-cc-pVDZ MRCI*+$[2]_{R12}$ errors are larger (ACT-1 error: 0.161 eV, ACT-2

Table 1. MRCI Electron Affinities of F Atom (eV) Computed As the Energy Difference between F Atom and F^- Anion[a]

method	active space	basis set	MRCI	MRCI + $[2]_{R12}$	MRCI + $[2]_{R12}$ + $[2]_S$	MRCI*[b] + $[2]_{R12}$
MRCI	ACT-1	aDZ	3.224	3.384	3.366	3.231
		aTZ	3.277	3.355	3.322	3.346
		aQZ	3.334	3.350	3.344	3.350
		CBS	3.392			
	ACT-2	aDZ	3.235	3.421	3.390	3.264
		aTZ	3.302	3.392	3.360	3.375
		aQZ	3.364	3.400	3.393	3.400
		CBS	3.427			
	ACT-3	aDZ	3.238	3.403	3.373	3.226
		aTZ	3.306	3.368	3.327	3.355

[a]"aXZ" refers to the aug-cc-pVXZ basis set. The CCSD + F12 + "high level correction" is 3.427 eV.[41] [b]Computed as E_{CASSCF}(aQZ) plus (E_{MRCI}-E_{CASSCF}) in the given basis set.

dx.doi.org/10.1021/ct4006773 | J. Chem. Theory Comput. 2014, 10, 90−101

Table 2. MRMP2 Electron Affinities of F Atom (eV) Computed by the Energy Difference between F Atom and F^- Anion[a]

method	active space	basis set	MRMP2	MRMP2 + $[2]_{R12}$	MRMP2 + $[2]_{R12}$ + $[2]_S$	MRMP2*[b] + $[2]_{R12}$
MRMP2	ACT-1	aDZ	3.167	3.353	3.334	3.200
		aTZ	3.199	3.306	3.273	3.296
		aQZ	3.251	3.302	3.296	3.302
		CBS	3.306			
	ACT-2	aDZ	3.122	3.350	3.319	3.193
		aTZ	3.151	3.274	3.242	3.257
		aQZ	3.202	3.262	3.255	3.262
		CBS	3.257			
	ACT-3	aDZ	3.123	3.329	3.299	3.153
		aTZ	3.157	3.269	3.230	3.256
		aQZ	3.205	3.259	3.252	3.259
		CBS	3.259			

[a]"aXZ" refers to the aug-cc-pVXZ basis set. The CCSD+F12+"high level correction" is 3.427 eV.[39]. [b]Computed as E_{CASSCF}(aQZ) plus (E_{MRMP2}-E_{CASSCF}) in the given basis set.

error: 0.163 eV) than the MRCI+$[2]_{R12}$+$[2]_S$ values (ACT-1 error: 0.026 eV, ACT-2 error: 0.037 eV).

Table 2 displays MRMP2 EAs of F atom for the ACT-1, ACT-2, and ACT-3 active spaces (see Supporting Information, Tables 4−6 for the total energy values). As the basis set size is increased the MRMP2 EAs approach the CBS limits for each active space (3.306 eV, 3.257 eV, and 3.259 eV, respectively). Compared to conventional MRMP2, the MRMP2+$[2]_{R12}$ and MRMP2+$[2]_{R12}$+$[2]_S$ predicted EAs lie much closer to the CBS estimates. The MRMP2+$[2]_{R12}$ and MRMP2+$[2]_{R12}$+$[2]_S$ EAs are overestimated when treated with the aug-cc-pVDZ basis set, but the EAs do converge to the CBS limit as the size of the AO basis is increased. For the MRMP2+$[2]_{R12}$+$[2]_S$ method, there is an oscillation in the sign of the EA error as the CBS limit is approached. The MRMP2*+$[2]_{R12}$ predicted EAs behave similarly to those predicted by MRCI*+$[2]_{R12}$—the aug-cc-pVDZ error is larger, while the aug-cc-pVTZ and aug-cc-pVQZ results are nearly converged to the extrapolated CBS estimates.

MRMP2 EAs do not show the same agreement with experiment as do the MRCI EAs (exp. 3.401 eV). However the convergence of the predicted EAs compared to the CBS limits is faster when the $[2]_{R12}$ and $[2]_S$ corrections are considered. The $[2]_S$ BSIE correction adds little improvement to the EAs compared to MRMP2 + $[2]_{R12}$. There does not appear to be a significant difference in the predicted EA values obtained from the various active spaces used.

Conformations of Si_2H_4. As a result of the relative weakness of silicon π-bonds, unsaturated silicon hydrides have many physical dissimilarities compared to analogous hydrocarbons.[43] The Si_2H_4 ground state aug-cc-pVDZ MRMP2 optimized structure has C_s symmetry while the transition state connected to the minimum energy structure has C_{2v} symmetry (Figure 1).

A (2,2) active space (π and π^* orbitals) is used for the CASSCF wave function. All conformer energies are computed at the aug-cc-pVDZ MRMP2 optimized geometries. In the minimum energy structure, the π and π^* orbitals have natural orbital occupation numbers of approximately 1.82 and 0.18 (respectively), suggesting significant multireference character.[44] Table 3 displays the energy differences between the C_{2v} and C_s conformers at the conventional and explicitly correlated MRMP2 and MRCI levels of theory (see Supporting Information, Tables 7−10 for total energy values). The MRMP2 energies were computed with the aug-cc-pVDZ, aug-cc-pVTZ, and aug-cc-pVQZ basis sets. Because of the physical memory requirements for the pilot-quality $[2]_{R12}$ and $[2]_S$ implementations in MPQC, the MRCI $[2]_{R12}$ and $[2]_S$ corrections are computed with the aug-cc-pVDZ basis only. The number of orbitals that are explicitly correlated (N_{corr} − geminal orbitals) is set to either 2 (active orbitals only) or 12 (all valence orbitals); N_{corr} is indicated in Table 3.

For the basis sets used, the conventional MRMP2 and MRCI methods overestimate the energy difference between conformers (error range ∼0.47−0.09 kcal/mol) compared to the CBS limit. MRMP2+$[2]_{R12}$ reduces the error range to 0.22−0.09 kcal/mol (0.35−0.07 kcal/mol) when 7 (2) strongly occupied valence orbitals are explicitly correlated. The conformer energy differences relative to the CBS limit are underestimated (overestimated) when 7 (2) orbitals are explicitly correlated. MRCI + $[2]_{R12}$ overestimates (underestimates) the conformer energy difference by 0.33 kcal/mol (0.15 kcal/mol) when 2 (7) orbitals are explicitly correlated. MRCI predicts a larger C_{2v} − C_s energy difference than that predicted by MRMP2 (∼2 kcal/mol larger). However, it is important to note that all of the energy differences are rather small and that the $[2]_{R12}$ method always corrects the energy so that the error with respect to the CBS limit is smaller.

C_2 Potential Energy Surfaces. Accurate calculations of excited electronic states can be difficult in ab initio electronic structure methods since the excited states, unlike most ground states, are frequently dominated by more than one configuration. This is especially true for bond dissociations, for which several configurations and/or states can mix at different points along the PES. The C_2 molecule is a notoriously challenging benchmark test for multireference methods, because even ground state C_2 is strongly multireference. The ground state C_2 wave function can be qualitatively characterized as having two π bonding orbitals and minimal σ bonding character. Notable reference studies of C_2 include a full CI determination of the PES with the 6-31G (d) basis set[45] and an MRCI analysis of the PES with the correlation consistent cc-pVXZ basis sets (up to X = 5).[46] The purpose of this subsection is to examine the performance of the $[2]_{R12}$ and $[2]_S$ BSIE corrections along the dissociation PES for the ground and the three lowest excited states of C_2 (two singlets and two triplets).

The CASSCF reference wave function for C_2 is constructed with eight electrons and the eight valence (1σ, $1\sigma^*$,1π,$1\pi^*$$2\sigma$,$2\sigma^*$) molecular orbitals (Figure 2). The two carbon 1s orbitals are constrained to be doubly occupied in the CASSCF and MRCI computations. MRCI is used to construct the PESs for the four

dx.doi.org/10.1021/ct4006773 | J. Chem. Theory Comput. 2014, 10, 90−101

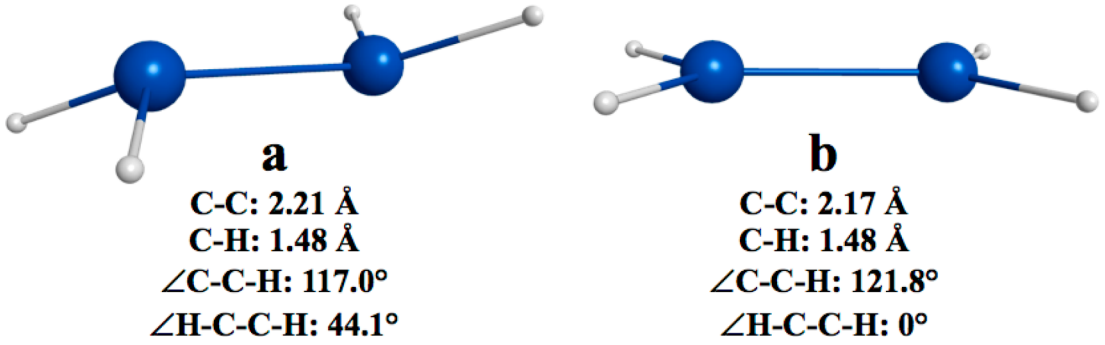

Figure 1. Si_2H_4 aug-cc-pVDZ MRMP2 optimized geometry of (a) the ground state (C_s) and (b) the transition state (C_{2v}).

Table 3. Conventional and Explicitly Correlated MRCI and MRMP2 Energy Differences (kcal/mol) between the Minimum and Transition State Structures of Si_2H_4[a]

N_{corr}	basis set	MRMP2	MRMP2 + $[2]_{R12}$	MRMP2 + $[2]_{R12}$ + $[2]_S$	MRMP2*[b] + $[2]_{R12}$	MRCI	MRCI + $[2]_{R12}$	MRCI $[2]_{R12}$ + $[2]_S$	MRCI*[b] + $[2]_{R12}$
2	aDZ	1.49	1.22	1.04	1.21	3.43	3.29	3.12	3.29
	aTZ	1.25	1.08	1.06	1.05	3.17			
	aQZ	1.03	0.94	0.94	0.94	3.06			
	CBS	0.87				2.96			
12	aDZ	1.49	0.65	0.47	0.64	3.43	2.81	2.63	2.81
	aTZ	1.25	0.77	0.75	0.74	3.17			
	aQZ	1.03	0.78	0.78	0.78	3.06			
	CBS	0.87				2.96			

[a] N_{corr} is the number of molecular orbitals (geminal orbitals) explicitly correlated in the $[2]_{R12}$ computation. "aXZ" refers to the aug-cc-pVXZ basis set. [b] Computed as E_{CASSCF}(aQZ) plus ($E_{MRMP2} - E_{CASSCF}$) or ($E_{MRCI} - E_{CASSCF}$) in the given basis set.

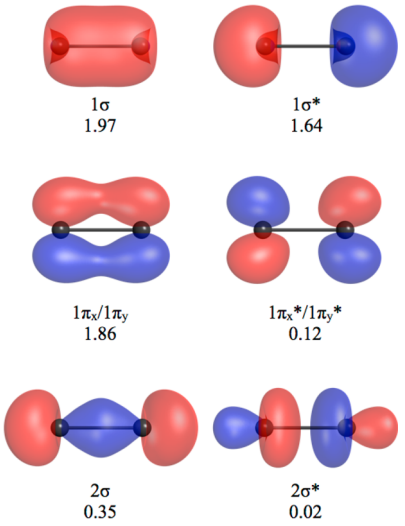

Figure 2. Molecular orbitals of C_2 that are used to construct the MCSCF active space. The MCSCF natural orbital occupation numbers are shown below the orbital designations.

lowest energy states (X $^1\Sigma_g^+$, a $^3\Pi_u$, b $^3\Sigma_g^-$, and A $^1\Pi_u$) of C_2 for which comprehensive spectroscopic data is available.[47,48] The D_{2h} point group is used for all computations (see Tables 11−14 in Supporting Information for total energy values) and density fitting is used for integral evaluation in the MPQC program for the $[2]_{R12}$ and $[2]_S$ aug-cc-pVQZ results.

The PESs were computed by varying the internuclear distance from 0.8 to 6.0 Å. Three grids (coarse, medium, fine) were used to determine the PES for each state. A course grid was obtained in intervals of 0.125 Å to establish the general features of the surface. A medium grid was obtained in intervals of 0.01 Å around the equilibrium bond distance. A fine grid, steps of 0.001 Å, was used to refine the equilibrium distance.

Table 4 displays the electronic dissociation energies D_e (kcal/mol), the adiabatic electronic excitation energies (differences between the ground and excited state minima) T_e (cm^{-1}), and the equilibrium bond lengths R_e (Å) for the $X^1\Sigma_g^+$, $a^3\Pi_u$, $b^3\Sigma_g^-$, and $A^1\Pi_u$ states. Table 4 includes results that were obtained using both conventional and explicitly correlated MRCI computations. The explicitly correlated results include the $[2]_{R12}$ and $[2]_S$ BSIE corrections.

As the cardinal number of the basis set is increased, the conventional MRCI predictions (in general) for the $X^1\Sigma_g^+$, $a^3\Pi_u$, and $b^3\Sigma_g^-$ states change monotonically, and converge toward the experimental values. For the $A^1\Pi_u$ state, as the cardinal number of the basis set is increased the conventional MRCI D_e energies and equilibrium bond lengths converge toward the experimental values, however the excitation energy overshoots the experimental value. Similar behavior was seen for the non-augmented correlation consistent basis sets when the contracted MRCI (CMRCI) method was used to examine the $a^3\Pi_u$ state.[46] Unlike the CMRCI study,[46] the conventional MRCI (aug-cc-pVXZ, X = D,T,Q) T_e values computed here approach the experimental measurements for the $a^3\Pi_u$ state as the cardinal number of the basis set is increased. In all cases, the equilibrium distances shorten and the D_e values increase with the cardinal number of the basis set. The adiabatic excitation energies tend to increase with increasing basis set size except for the MRCI*, MRCI*+$[2]_{R12}$, and MRCI+$[2]_{R12}$+$[2]_S$ values for the $A^1\Pi_u$ state. There is a slight oscillation with the MRCI +$[2]_{R12}$+$[2]_S$ T_e values for the $a^3\Pi_u$ state.

In comparison to conventional MRCI, the MRCI+$[2]_{R12}$ and MRCI+$[2]_{R12}$+$[2]_S$ predicted dissociation energies and excitation energies improve relative to experiment as the basis set is increased. Only the MRCI/aug-cc-pVTZ T_e for the $A^1\Pi_u$ state is

dx.doi.org/10.1021/ct4006773 | J. Chem. Theory Comput. 2014, 10, 90−101

Table 4. Dissociation Energies (D_e, kcal/mol), Adiabatic Excitation Energies (T_e, cm^{-1}), and Equilibrium Bond Distances (R_e, Å) for C_2

State	Method	Basis set	D_e (kcal/mol)	T_e (cm^{-1})	R_e (Å)
$X^1\Sigma_g^+$					
	MRCI	aDZ	129.9	0	1.274
		aTZ	140.6	0	1.253
		aQZ	143.9	0	1.248
	MRCI*	aDZ	133.9	0	1.261
		aTZ	141.3	0	1.251
	MRCI + $[2]_{R12}$	aDZ	138.6	0	1.262
		aTZ	144.2	0	1.249
		aQZ	145.6	0	1.247
	MRCI* + $[2]_{R12}$	aDZ	143.0	0	1.248
		aTZ	144.9	0	1.247
	MRCI + $[2]_{R12}$ + $[2]_S$	aDZ	142.8	0	1.251
		aTZ	144.7	0	1.247
		aQZ	145.6	0	1.246
	Expt.[†]		147.8 ± 0.5	0	1.243
$a\ ^3\Pi_u$					
	MRCI	aDZ	130.1	−25.3	1.344
		aTZ	139.4	464.1	1.323
		aQZ	142.2	654.2	1.318
	MRCI*	aDZ	133.4	392.4	1.330
		aTZ	140.0	534.8	1.321
	MRCI + $[2]_{R12}$	aDZ	137.7	269.1	1.331
		aTZ	142.4	644.3	1.318
		aQZ	143.6	741.0	1.316
	MRCI* + $[2]_{R12}$	aDZ	141.2	709.1	1.318
		aTZ	143.0	715.2	1.318
	MRCI + $[2]_{R12}$ + $[2]_S$	aDZ	140.4	711.0	1.321
		aTZ	142.9	699.3	1.317
		aQZ	143.7	746.2	1.316
	Expt.[†]		145.8 ± 0.5	716.2	1.312
$b\ ^3\Sigma_g^-$					
	MRCI	aDZ	115.1	5198.7	1.399
		aTZ	123.5	6032.8	1.380
		aQZ	126.1	6300.9	1.375
	MRCI*	aDZ	117.7	5888.4	1.385
		aTZ	124.0	6151.8	1.378
	MRCI + $[2]_{R12}$	aDZ	122.4	5609.7	1.388
		aTZ	126.4	6236.7	1.376
		aQZ	127.4	6396.9	1.375
	MRCI* + $[2]_{R12}$	aDZ	125.2	6340.7	1.374
		aDZ	127.0	6356.1	1.374
	MRCI + $[2]_{R12}$ + $[2]_S$	aDZ	124.5	6299.8	1.377
		aTZ	126.9	6310.1	1.374
		aQZ	127.5	6397.2	1.375
	Expt.[†]		129.4 ± 0.5	6434.2	1.369
$A\ ^1\Pi_u$					
	MRCI	aDZ	106.7	8153.5	1.351
		aTZ	116.7	8399.2	1.329
		aQZ	119.8	8500.4	1.325
	MRCI*	aDZ	109.9	8615.2	1.337
		aTZ	117.3	8477.5	1.327
	MRCI + $[2]_{R12}$	aDZ	115.3	8086.7	1.339
		aTZ	120.2	8427.5	1.325
		aQZ	121.3	8522.0	1.323
	MRCI* + $[2]_{R12}$	aDZ	118.8	8570.9	1.325
		aTZ	120.8	8506.0	1.323
	MRCI + $[2]_{R12}$ + $[2]_S$	aDZ	118.0	8574.2	1.329
		aTZ	120.7	8483.8	1.323
		aQz	121.4	8528.6	1.323
	Expt.[†]		123.8 ± 0.5	8391.0	1.318

[*]Computed as E_{CASSCF}(aQZ) plus (E_{MRCI}-E_{CASSCF}) in the given basis set. [†]Experimental dissociation energy (D_e) taken from ref 47., T_e, and R_e taken from ref 48.

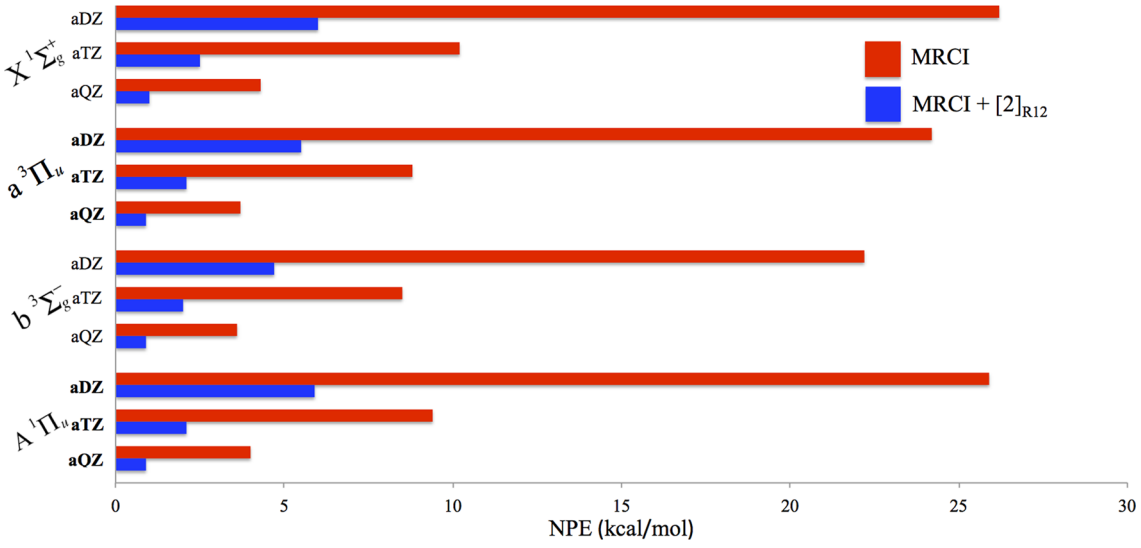

Figure 3. Nonparallelity errors (NPE) in the correlation energy for the $X\ ^1\Sigma_g^+$, $a^3\Pi_u$, $b^3\Sigma_g^-$, and $A^1\Pi_u$ states of C_2 (0.9−6.0 Å). MRCI and MRCI+$[2]_{R12}$ NPE errors are presented for aug-cc-pVXZ (X = D,T,Q) basis sets.

in closer agreement with experiment (absolute error ∼8 cm^{-1}) than are the explicitly correlated results (absolute error ∼21−304 cm^{-1}). The negative MRCI/aug-cc-pVDZ T_e excitation energy for the $a^3\Pi_u$ state (−24.3 cm^{-1}) indicates that the ground

dx.doi.org/10.1021/ct4006773 | J. Chem. Theory Comput. 2014, 10, 90−101

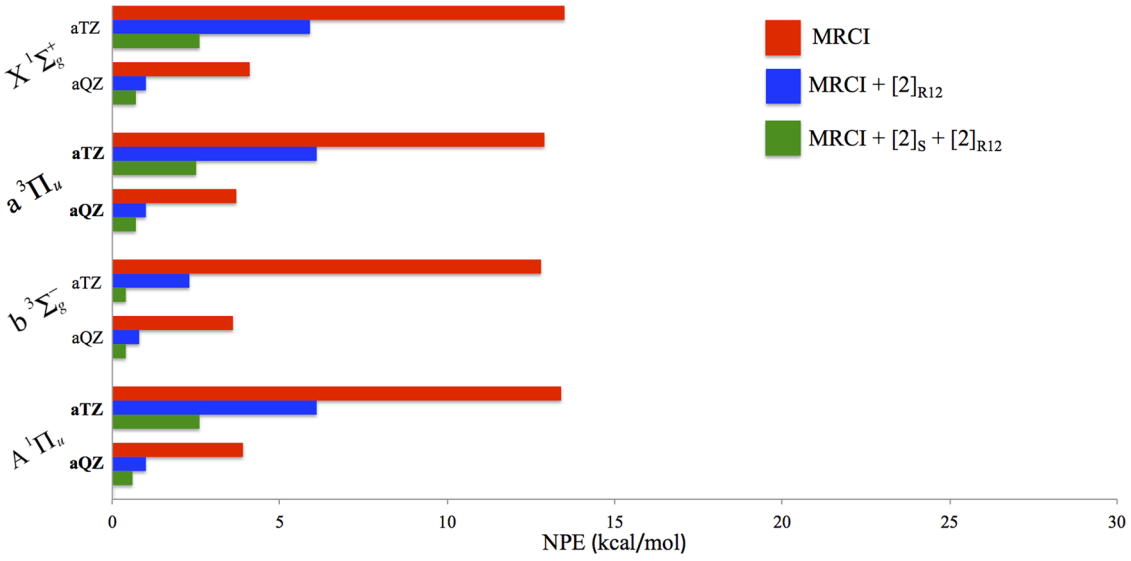

Figure 4. Nonparallelity errors (NPE) in the total energy for the $X^1\Sigma_g^+$, $a^3\Pi_u$, $b^3\Sigma_g^-$, and $A^1\Pi_u$ states of C_2 (0.9−6.0 Å). MRCI and MRCI+$[2]_{R12}$ NPE errors are presented for aug-cc-pVXZ (X = T,Q) basis sets.

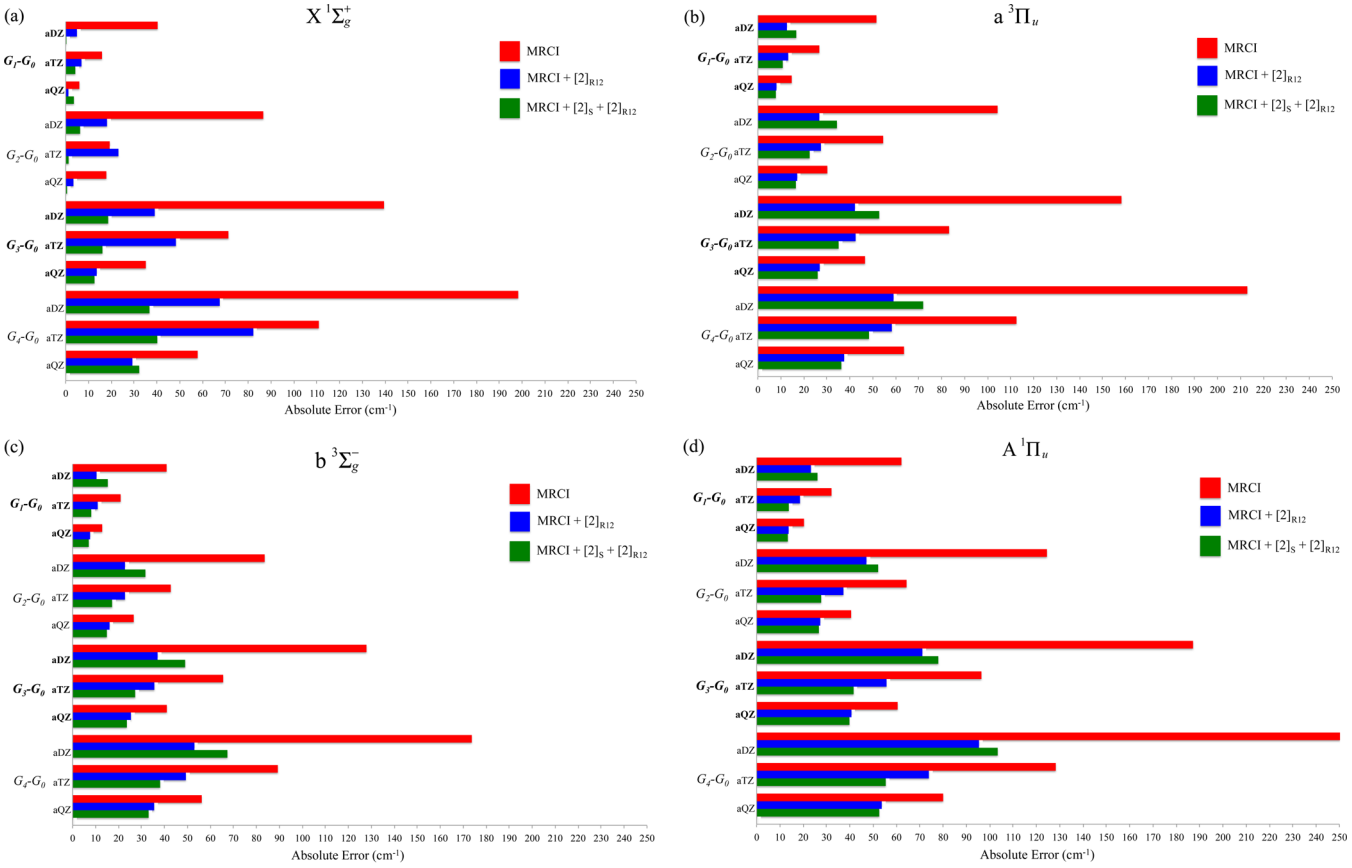

Figure 5. Errors (cm^{-1}) in the vibration energy level differences computed for (a) the X $^1\Sigma_g^+$ C_2 ground state, (b) the $a^3\Pi_u$ C_2 excited state, (c) the $b^3\Sigma_g^-$ C_2 excited state, and (d) the $A^1\Pi_u$ C_2 excited state. "aXZ" refers to the aug-cc-pVXZ basis set (X = D,T,Q). Errors are relative to experimental values taken from ref 48.

state ($X^1\Sigma_g^+$) is predicted to be higher in energy at this level of theory. The correct order of the $a^3\Pi_u$ and $X^1\Sigma_g^+$ states is predicted once explicit correlation is used. However, the BSIE error for this case is largely caused by the one-electron incompleteness since the error in the MRCI*/aug-cc-pVDZ T_e is smaller than the MRCI+$[2]_{R12}$ error. On average, the explicitly correlated MRCI/aug-cc-pVXZ results are in better agreement with experiment than are the conventional MRCI/aug-cc-pV(X+1)Z predictions, where X = D,T.

The nonparallelity errors (NPE) along the state-specific PESs (0.9−6.0 Å) for the $X^1\Sigma_g^+$, $a^3\Pi_u$, $b^3\Sigma_g^-$, and $A^1\Pi_u$ states are shown in Figures 3 and 4 (see Table 9 in Supporting

dx.doi.org/10.1021/ct4006773 | J. Chem. Theory Comput. 2014, 10, 90−101

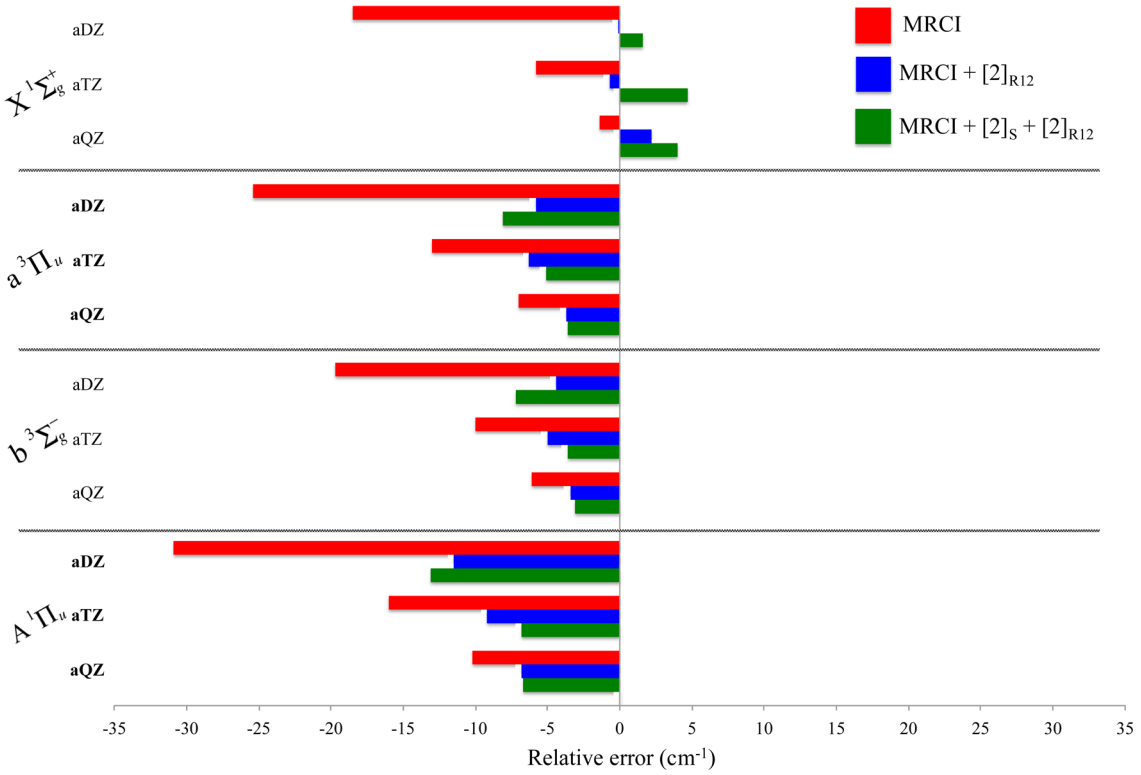

Figure 6. Error in C_2 zero-point energies (ZPE, cm^{-1}) determined from potential energies surfaces computed by MRCI, MRCI + $[2]_{R12}$, and MRCI + $[2]_{R12}$ + $[2]_S$. "aXZ" refers to the aug-cc-pVXZ basis set (X = D,T,Q). Errors are relative to experimental values taken from ref 47.

Information for numerical values for the NPEs). The NPE is defined as the difference between the maximum and the minimum errors in the energy with respect to the extrapolated CBS PES. Ideally, the NPE should be zero. The NPE in the correlation energy is examined to isolate the effects of the $[2]_{R12}$ correction. For MRCI+$[2]_{R12}$, a correlation energy NPE of 6.0−4.7 kcal/mol is seen among the states when the aug-cc-pVDZ basis set is used. The MRCI+$[2]_{R12}$ NPE is reduced to 2.5−2.0 kcal/mol when the aug-cc-pVTZ basis set us used. MRCI+$[2]_{R12}$ NPEs computed with the aug-cc-pVQZ basis set have a correlation energy NPE $\leq$ 1.0 kcal/mol. The NPEs in the total energy for the aug-cc-pVXZ (X = T,Q) are represented by Figure 4. The NPE error in the total energy for the aug-cc-pVTZ basis set is larger than the NPE in the correlation energy. These errors likely originate from the BSIE in the reference energy, since the NPE in the total energy decreases when the $[2]_S$ correction is included. The MRCI+$[2]_{R12}$+$[2]_S$ NPEs in the total energy range from 2.3 to 2.6 kcal/mol and 0.4−0.7 kcal/mol for the aug-cc-pVTZ and aug-cc-pVQZ basis sets, respectively.

A recent explicitly correlated full configuration interaction quantum Monte Carlo +$[2]_S$ +$[2]_{R12}$ (FCIQMC-F12) study examined the PES of the $X^1\Sigma_g^+$ C_2 ground state from R = 0.9−1.6 Å.[23] An additional study used the phaseless auxiliary-field quantum Monte Carlo (AFQMC) method to also examine the $X^1\Sigma_g^+$ C_2 ground state PES (0.9−3.0 Å).[49] The FCIQMC-F12 method used the cc-pVDZ basis set, while AFQMC used the 6-31G(d) basis set with a CASSCF trial wave function. Although these basis sets are different than those used in this study, they are still of double-ζ quality and provide a reasonable comparison for the aug-cc-pVDZ results in this work. The FCIQMC-F12 results show a NPE of 12.3 mh (in the range R = 0.9−1.6 Å) while MRCI+$[2]_{R12}$+$[2]_S$ shows an NPE of 13.9 mh (in the range R = 0.9−1.625 Å). The AFQMC study has an NPE of 7 mh (in the range R = 0.9−3.0 Å), while MRCI+$[2]_{R12}$+$[2]_S$ has a NPE of 14.8 mh over the same range.

The C_2 vibrational energy levels are obtained from solutions to the nuclear Schrödinger equation. These solutions are found by a discrete variable representation procedure[50] in which the potential energy curves are fitted to even-tempered Gaussians.[51] Details of the implementation are described elsewhere.[52] The first four experimental vibrational energy level differences ($G(\nu)$=G_ν-G_0, ν = 1,4) for the $X^1\Sigma_g^+$, $a^3\Pi_u$, $b^3\Sigma_g^-$, and $A^1\Pi_u$ states are shown in Figure 5 (see Table 11 in Supporting Information for numerical values). Relative to the experimental vibrational energy level differences,[47] the errors in the vibrational energy level differences computed by MRCI, MRCI+$[2]_{R12}$, and MRCI + $[2]_{R12}$+$[2]_S$ are of interest. Relative to experiment, the MRCI+$[2]_{R12}$ errors in vibrational energy differences for the $X^1\Sigma_g^+$, $a^3\Pi_u$, $b^3\Sigma_g^-$, and $A^1\Pi_u$ states are generally smaller compared to the MRCI errors. For the $a^3\Pi_u$, $b^3\Sigma_g^-$, and $A^1\Pi_u$ states aug-cc-pVTZ MRCI+$[2]_{R12}$+$[2]_S$ results show improvement over the MRCI+$[2]_{R12}$ results, however when the aug-cc-pVDZ basis set is used the opposite trend is seen. The lower vibrational energy level differences tend to be well represented in both the ground and excited states. The MRCI+$[2]_{R12}$ errors in the vibrational energy level differences do not asymptotically decrease with basis set size for the $X^1\Sigma_g^+$ as is seen (in general) for the excited states. Lastly the MRCI+$[2]_{R12}$ errors increase as ν increases because the fundamentals are off by some amount, hence for each higher level the deviation from the exact value will increase with ν.

The errors in the zero-point energies (ZPEs) for the $X^1\Sigma_g^+$, $a^3\Pi_u$, $b^3\Sigma_g^-$, and $A^1\Pi_u$ states computed with aug-cc-pVXZ (X = D,T,Q) relative to the experimental ZPEs[47] are presented in

dx.doi.org/10.1021/ct4006773 | J. Chem. Theory Comput. 2014, 10, 90−101

Figure 6 (see Table 11 in Supporting Information for numerical values). Overall, the aug-cc-pVXZ (X = D,T,Q) MRCI +$[2]_{R12}$ predicted ZPE agrees better with experiment than MRCI alone. The only exception to this trend is the aug-cc-pVQZ MRCI+$[2]_{R12}$ value for the $X^1\Sigma_g^+$ state. The unsigned error (compared to experiment) for the MRCI+$[2]_{R12}$ value (1.4 cm^{-1}) is slightly larger than the unsigned error in the conventional MRCI value (1.1 cm^{-1}). Compared to the MRCI+$[2]_{R12}$ ZPEs, the MRCI+$[2]_{R12}$+$[2]_S$ ZPEs exhibit minor differences (~1−3 cm^{-1}).

Sample Timings for the Pilot Code. To provide a preliminary idea of the expense of the calculations, timing information for the pilot code has also been collected in Table 5 for the C_2 molecule for MRCI and MRMP2 single point energies in D_{2h} symmetry. The size of the OBS and CABS basis sets are shown along with the amount of time (in minutes) for each CI iteration or full MRMP2 energy computation, 2-RDM generation, $[2]_{R12}$ correction, and $[2]_S$ correction. All computations were carried out in serial on an Intel Xeon E2690 processor.

Table 5. Timing Comparisons for MRCI and MRMP2 C_2 Computations[a]

method/basis set	size of OBS	size of CABS	energy[b] (min)	2-RDM (min)	$[2]_{R12}$ (min)	$[2]_S$ (min)
MRCI/aDZ	46	138	0.1	0.2	0.3	0.2
MRCI/aTZ	92	156	2.2	2.5	1.4	0.4
MRCI/aQZ	160	178	9.1	19.9	10.8	1.0
MRMP2/aDZ	46	138	<0.1	<0.1	0.2	0.2
MRMP2/aTZ	92	156	0.1	<0.1	0.4	0.4
MRMP2/aQZ	160	178	0.4	<0.1	1.4	1.0

[a]Timing results are given for one CI iteration or the MRMP2 computation, 2-RDM computation, $[2]_{R12}$, and $[2]_S$. All timings were run in serial on an Intel Xeon E5-2690 processor. [b]The full cost of the MRMP2 computation or one CI iteration.

Since the 2-RDM from the CASSCF is used for the MRMP2 computations, the 2-RDM has already been calculated for the MRMP2 computation and there is no extra cost associated with its formation. However, for MRCI, there is an additional cost associated with the 2-RDM formation. While the cost to form the 2-RDM is higher than the cost of a CI iteration, it must be kept in mind that it is often the case that 30 or more CI iterations are required for convergence. Therefore the cost to form the 2-RDM is lower than that of the CI calculation. In addition, the 2-RDM formation has been parallelized across nodes (both for memory and CPU considerations) and so the formation time will decrease significantly with the addition of processes. However, whenever the parallel 2-RDM code is used, an expensive sort operation is required, so that data can be efficiently transferred between nodes and processes. For example, if the aug-cc-pVQZ 2-RDM is computed in serial with the entries sorted, the CPU time is 48.3 min vs 19.9 min for the unsorted entries. When the 2-RDM computation with the sort is run in parallel with 2 cores, the time decreases to 25.3 min (~1.9× speedup compared to a single core), and with eight cores there is a ~7.1× speedup.

CONCLUSION

This paper reports an assessment of the explicitly correlated $[2]_{R12}$ correction for the BSIE of the electron correlation energy, and its sister $[2]_S$ correction for the BSIE of the reference energy. The $[2]_{R12}$ correction was formulated in this work such that only strongly occupied (inactive + active) orbitals in the reference MRCI or CASSCF wave function are correlated, thus the computational cost of this formulation is comparable to that of MP2-R12. Consequently, this implementation MRCI-R12 methodology is amenable to larger molecular systems (e.g., Si_2H_4) than have previously been accessible for this method.

All computations in this work utilized the new interface between the GAMESS and MPQC electronic structure codes. GAMESS is used to compute the CASSCF or MRCI wave function and the second-order reduced density matrix. MPQC then uses the second-order reduced density matrix, the CASSCF orbitals, the nuclear coordinates, and the basis set information from GAMESS to compute the $[2]_{R12}$ and $[2]_s$ BSIE corrections.

For F atom, the MRCI + $[2]_{R12}$ EAs computed with the aug-cc-pVDZ basis set are consistent with the conventional MRCI CBS estimates. The MRMP2 + $[2]_{R12}$ EAs computed with the aug-cc-pVDZ basis set are within 0.05 eV of the MRMP2 CBS estimates. The $[2]_S$ correction and the MRCI* + $[2]_{R12}$ EAs offer significant improvement of the predicted MRCI and MRCI + $[2]_{R12}$ EAs for F atom.

For the two Si_2H_4 conformers, the conventional MRCI (MRMP2) CBS limit indicates that the C_s conformer is 3.0 (0.9) kcal/mol lower in energy than the planar C_{2v} structure. When only two active orbitals are explicitly correlated, MRMP2 + $[2]_{R12}$ predicts conformer energy differences with the aug-cc-pVXZ basis set that are comparable to the energy differences that are obtained using the aug-cc-pV(X+1)Z basis set with the conventional MRMP2 computation (X = D,T). For example, MRMP2 + $[2]_{R12}$ using the aug-cc-pVDZ basis set predicts a conformer energy difference of 1.22 kcal/mol, which is comparable with the conventional MRMP2 value of 1.25 kcal/mol using the aug-cc-pVTZ basis set. When all 7 occupied valence orbitals are explicitly correlated, the energy differences converge rapidly toward the extrapolated CBS result. Although the conformer energy difference of 2.81 kcal/mol is larger for MRCI + $[2]_{R12}$, MRCI + $[2]_{R12}$ shows similar behavior of the energy differences compared to the MRMP2 + $[2]_{R12}$ method.

The MRCI + $[2]_{R12}$ results for C_2 show significant improvements over conventional MRCI computations. MRCI + $[2]_{R12}$ is well suited to obtain accurate dissociation energies (D_e), minimum energy differences (T_e), and C−C equilibrium bond distances. The MRCI + $[2]_{R12}$ method also exhibits smaller NPEs than conventional MRCI. The $[2]_{R12}$ and $[2]_S$ corrections also show significant improvements over traditional MRCI for the vibrational energy level differences. The exception is that with the aug-cc-pVDZ basis set the $[2]_S$ correction results in larger errors for the excited states.

In summary, as has been seen with other studies, explicitly correlated MRCI relative energies computed with the aug-cc-pVXZ basis sets are typically better than results obtained from conventional MRCI methods computed with the aug-cc-pV(X+1)Z basis sets, where X = D,T,Q. The R12 corrected energy differences between the aug-cc-pVTZ and aug-cc-pVQZ basis sets are almost always much smaller than those without the R12 corrections. On the basis of the predictions for the systems studied here, the $[2]_S$ BSIE correction tends to speed up convergence of the reference energy as expected.

dx.doi.org/10.1021/ct4006773 | J. Chem. Theory Comput. 2014, 10, 90−101

■ ASSOCIATED CONTENT

Supporting Information

A descriptive explanation of the format used for the disk files written by GAMESS and read by MPQC is available. An example GAMESS input file, total energies for all calculations, and tabular information for the NPEs, vibrational energy errors, and zero point energies for C_2 are also included. This material is available free of charge via the Internet at http://pubs.acs.org.

■ AUTHOR INFORMATION

Corresponding Author

*E-mail: theresa@fi.ameslab.gov.

Present Address

[§]Department of Chemistry, Stanford University, Palo Alto, CA.

Notes

The authors declare no competing financial interest.

■ ACKNOWLEDGMENTS

Funding has been provided by an NSF SI2 grant (awards OCI-1047772 to ISU and OCI-1047696 to VT). The work by L.K. and E.F.V. was also supported by an NSF CAREER award (CHE-0847295), an NSF CRIF-MU award (CHE-0741927), and the Alfred P. Sloan Research Fellowship and the Camille and Henry Dreyfus Teacher-Scholar Award. The computations reported in this work were performed on computer clusters that were provided by the U.S. Department of Energy Office of Science (via the Ames Laboratory) and by the Air Force Office of Scientific Research. The authors are indebted to Dr. L. Bytautas for providing a copy of the PECfit.f program that was used to fit potential energy curves in terms of even-tempered Gaussian functions and Prof. N. Matsunaga for providing a discrete variable representation program to compute vibrational energy levels. L.B.R. thanks Prof. Kurt Peterson for insightful discussions.

■ REFERENCES

(1) Klopper, W.; Manby, F. R.; Ten-no, S.; Valeev, E. F. *Int. Rev. Phys. Chem.* **2006**, *25*, 427−468.

(2) Kutzelnigg, W.; Klopper, W. *J. Chem. Phys.* **1991**, *94*, 1985−2001.

(3) Kong, L.; Bischoff, F. A.; Valeev, E. F. *Chem. Rev.* **2012**, *112*, 75−107. Hättig, C.; Klopper, W.; Köhn, A.; Tew, D. P. *Chem. Rev.* **2012**, *112*, 4−74.

(4) Kong, L.; Valeev, E. F. *J. Chem. Phys.* **2011**, *135*, 214105.

(5) Valeev, E. F. *Chem. Phys. Lett.* **2004**, *395*, 190−195.

(6) Ten-no, S. *J. Chem. Phys.* **2004**, *121*, 117−129.

(7) Kedžuch, S.; Milko, M.; Noga, J. *Int. J. Quantum Chem.* **2005**, *105*, 929−936.

(8) Fliegl, H.; Klopper, W.; Hättig, C. *J. Chem. Phys.* **2005**, *122*, 84107.

(9) Torheyden, M.; Valeev, E. F. *Phys. Chem. Chem. Phys.* **2008**, *10*, 3410−3420.

(10) Adler, T. B.; Knizia, G.; Werner, H.-J. *J. Chem. Phys.* **2007**, *127*, 221106.

(11) Gdanitz, R. J. *Chem. Phys. Lett.* **1993**, *210*, 253−260. Gdanitz, R. J.; Röhse, R. *Int. J. Quantum Chem.* **1995**, *55*, 147−150. Gdanitz, R. J.; Röhse, R. *Int. J. Quantum Chem.* **1996**, *59*, 505E. Gdanitz, R. J. *Chem. Phys. Lett.* **1998**, *283*, 253−261. Gdanitz, R. J. *Chem. Phys. Lett.* **1998**, *288*, 590−592. Gdanitz, R. J. *Chem. Phys. Lett.* **1998**, *295*, 540E.

(12) Gdanitz, R. J.; Ahlrichs, R. *Chem. Phys. Lett.* **1998**, *143*, 413−420. Gdanitz, R. J. *Int. J. Quantum Chem.* **2001**, *85*, 281−300.

(13) Ten-no, S. *Chem. Phys. Lett.* **2007**, *447*, 175−179.

(14) Hirao, K. *Chem. Phys. Lett.* **1992**, *190*, 374−380. Hirao, K. *Chem. Phys. Lett.* **1992**, *196*, 397−403. Hirao, K. *Int. J. Quantum Chem.* **1992**, *S26*, 517−526.

(15) Shiozaki, T.; Werner, H.-J. *J. Chem. Phys.* **2010**, *133*, 141103.

(16) Shiozaki, T.; Knizia, G.; Werner, H.-J. *J. Chem. Phys.* **2011**, *134*, 034113.

(17) Mahapatra, U. S.; Datta, B.; Mukherjee, D. *Chem. Phys. Lett.* **1999**, *299*, 42−50. Mahapatra, U. S.; Datta, B.; Mukherjee, D. *J. Phys. Chem. A* **1999**, *103*, 1822−1830. Mao, S.; Cheng, L.; Liu, W.; Mukherjee, D. *J. Chem. Phys.* **2012**, *136*, 024105. Mao, S.; Cheng, L.; Liu, W.; Mukherjee, D. *J. Chem. Phys.* **2012**, *136*, 024106.

(18) Haunschild, R.; Mao, S.; Mukherjee, S.; Klopper, W. *Chem. Phys. Lett.* **2012**, *531*, 247−251.

(19) Haunschild, R.; Cheng, L.; Mukherjee, D.; Klopper, W. *J. Chem. Phys.* **2013**, *138*, 211101−211104.

(20) Liu, W.; Hanauer, M.; Köhn, A. *Chem. Phys. Lett.* **2013**, *565*, 122−127.

(21) Kedžuch, S.; Demel, O.; Pittner, J.; Ten-no, S.; Noga, J. *Chem. Phys. Lett.* **2011**, *418*, 511.

(22) Torheyden, M.; Valeev, E. F. *J. Chem. Phys.* **2009**, *131*, 171103.

(23) Booth, G. H.; Cleland, D.; Alavi, A.; Tew, D. P. *J. Chem. Phys.* **2012**, *137*, 164112−164122.

(24) White, S. R. *Phys. Rev. Lett.* **1992**, *69*, 2863.

(25) Yanai, T.; Shiozaki, T. *J. Chem. Phys.* **2012**, *136*, 084107.

(26) Gordon, M. S.; Schmidt, W. W. Advances in Electronic Structure Theory: GAMESS a Decade Later. In *Theory and Applications of Computational Chemistry*; Dykstra, C. E., Frenking, G., Kim, K. S., Scuseria, G. E., Eds.; Elsevier: Amsterdam, The Netherlands, 2005; Chapter 41. Schmidt, M. W.; Baldridge, K. K.; Boatz, J. A.; Elbert, S. T.; Gordon, M. S.; Jensen, J. J.; Koseki, S.; Matsunaga, N.; Nguyen, K. A.; Su, S.; Windus, T. L.; Dupuis, M.; Montgomery, J. A. *J. Comput. Chem.* **1993**, *14*, 1347−1363.

(27) Janssen, C. L.; Nielsen, I. B.; Leininger, M. L., Valeev, E. F.; Seidl, E. T. *The Massively Parallel Quantum Chemistry Program (MPQC)*, Version 3.0 (alpha); Sandia National Laboratories: Livermore, CA, 2009.

(28) Aquilante, F.; De Vico, L.; Ferré, N.; Ghigo, G.; Malmqvist, P.-Å.; Neogrády, P.; Pedersen, T. B.; Pitonak, M.; Reiher, M.; Roos, B. O.; Serrano-Andrés, L.; Urban, M.; Veryazov, V.; Lindh, R. *J. Comput. Chem.* **2010**, *31*, 224−247.

(29) Ten-no, S. *Chem. Phys. Lett.* **2004**, *398*, 56−61.

(30) Kong, L.; Valeev, E. F. *J. Chem. Phys.* **2010**, *133*, 174126.

(31) Dyall, K. *J. Chem. Phys.* **1995**, *102*, 4909−4918.

(32) Dunning, T. H., Jr. *J. Chem. Phys.* **1989**, *90*, 1007−1023.

(33) Halgaker, T.; Klopper, W.; Koch, H.; Noga, J. *J. Chem. Phys.* **1997**, *106*, 9639−9646.

(34) Klopper, W.; Kutzelnigg, W. *J. Mol. Struct.: THEOCHEM* **1986**, *135*, 339−356. Kutzelnigg, W. *Int. J. Quantum Chem.* **1994**, *51*, 447−463.

(35) Feller, D. *J. Chem. Phys.* **1992**, *96*, 6104−6114.

(36) Gdantiz, R. J. *J. Chem. Phys.* **1999**, *110*, 706−710.

(37) de Oliveira, G.; Martin, J. M. L.; de Proft, F.; Geerlings, P. *Phys. Rev. A* **1999**, *60*, 1034−1045.

(38) Li, J.; Zhao, Z.; Andersson, M.; Zhang, X.; Chen, C. *J. Phys. B.: At., Mol. Opt. Phys.* **2012**, *45*, 165004.

(39) Gdanitz, R. J. *Chem. Phys. Lett.* **1998**, *283*, 253−261.

(40) Gdantiz, R. J. *J. Chem. Phys.* **1998**, *109*, 9795−9801.

(41) Klopper, W.; Bachorz, R. A.; Tew, D. P.; Hättig, C. *Phys. Rev. A* **2010**, *81*, 022503−022508.

(42) Blondel, C.; Delsart, C.; Goldfarb, F. *J. Phys. B: Atom. Mol. Opt. Phys.* **2001**, *34*, L281−L288.

(43) Teo, B. K.; Sun, X. H. *Chem. Rev.* **2007**, *107*, 1454−1532.

(44) Gordon, M. S.; Schmidt, M. W.; Chaban, G. M.; Glaesemann, K. R.; Stevens, W. J.; Gonzalez, C. *J. Chem. Phys.* **1999**, *110*, 4199−4207.

(45) Abrams, M.; Sherrill, D. *J. Chem. Phys.* **2004**, *121*, 9211−9219.

(46) Peterson, K. A. *J. Chem. Phys.* **1995**, *102*, 262−277.

(47) Urdahl, R. S.; Bao, Y.; Jackson, W. M. *Chem. Phys. Lett.* **1991**, *178*, 425−428.

(48) Huber, K. P.; Herzberg, G. *Molecular Spectra and Molecular Structure IV. Constants of Diatomic Molecules*; Van Nostrand: Princeton, NJ, 1979.

(49) Purwanto, W.; Zhang, S.; Krakauer, H. *J. Chem. Phys.* **2009**, *130*, 094107−094115.
(50) Colbert, D. T.; Miller, W. H. *J. Chem. Phys.* **1992**, *96*, 1982−1991.
(51) Bytautas L., program PECfit.f for fitting potential energy curves in terms of even-tempered Gaussian functions.
(52) Bytautas, L.; Matsunaga, N.; Ruedenberg, K. *J. Chem. Phys.* **2010**, *132*, 074307−074321. Bytautus, L.; Matsunaga, N.; Nagata, T.; Gordon, M. S.; Ruedenberg, K. *J. Chem. Phys.* **2007**, *127*, 204313−204331.